Extremal Transmission and Beating Effect of Acoustic Waves in Two-Dimensional Sonic Crystals

Xiangdong Zhang[1] and Zhengyou Liu[2]

[1]*Department of Physics, Beijing Normal University, Beijing 100875, China*

[2]*Key Lab of Acoustic and Photonic Materials and Devices of Ministry of Education, Wuhan University, Wuhan 430072, China and Department of Physics, Wuhan University, Wuhan 430072, China*

(Received 21 March 2008; revised manuscript received 2 October 2008; published 30 December 2008)

The extremal transmission of the acoustic wave near the Dirac point in two-dimensional (2D) sonic crystals, being inversely proportional to the thickness of sample, has been demonstrated experimentally for the first time. Some unusual beating effects have been observed experimentally, when the acoustic pulse transports through the 2D sonic crystal slabs. Such phenomena are completely different from the oscillations of the wave in a slab or cavity originating from the interface reflection or the Fabry-Perot effect. They can be regarded as an acoustic analogue effect to *Zitterbewegung* of the relativistic electron. The physical origination for the phenomenon has been analyzed.

DOI: 10.1103/PhysRevLett.101.264303 PACS numbers: 43.35.+d, 63.20.−e

Recently, there has been a great deal of interest in studying the transport of electromagnetic waves near the Dirac point in two-dimensional (2D) photonic crystals (PCs) [1–3]. In some 2D PCs with triangular or honeycomb lattices, the band gap may become vanishingly small at the corners of the Brillouin zone, where two bands touch as a pair of cones. Such a conical singularity is referred to as the Dirac point, similar to the case of electrons in the monolayer graphene [4,5]. When we describe the transport of electromagnetic waves near the Dirac point inside the PCs, the Maxwell equations can be reduced to the Dirac equation due to the linear dispersion around it [1]. This leads to some unusual transmission properties of electromagnetic waves in the PCs [1–3]. For example, the optical conductance near the Dirac point is inversely proportional to the thickness of the sample, which is different from the ballistic behavior in general band regions and exponential decay in the gap regions with the increase of sample thickness [2]. Although such an extremal transmission phenomenon in the 2D PCs has been pointed out theoretically [2], it has not been observed experimentally so far.

In this work, we demonstrate both experimentally and theoretically that such a phenomenon can also appear for acoustic waves in the 2D sonic crystals (SCs). Based on these, we then studied experimentally the dynamic behavior of pulse transmission through the 2D SC slabs with the center frequency near the Dirac point. Some unusual beating effects were found. The phenomenon can be regarded as an acoustic analogue to the *Zitterbewegung* (ZB) of the relativistic electron, which is similar to the case of the photon near the Dirac point in the PCs [3].

The SC used in the experiments consists of a hexagonal array of steel cylinders immersed in water with a lattice constant $a = 1.5$ mm and a filling ratio 0.403. The band structure of the system obtained by the multiple-scattering Korringa-Kohn-Rostoker method [6] is shown in Fig. 1(a). The material parameters used in the calculations are, for water, density $\rho = 1000\ \mathrm{g/m^3}$ and sound velocity $c = 1490$ m/s and, for steel, density $\rho = 7800\ \mathrm{g/m^3}$ and longitudinal wave velocity $c_l = 6010$ m/s. The corresponding measured data of the transmission coefficient along the ΓK direction for a rectangular sample with a different thickness and width 86 mm are plotted in Fig. 1(b). The measurement, based on the well-known ultrasonic transmission technique [7], is performed on a Panametrics LSC-02 ultrasonic scanning system. A pulser-receiver generator (Panametrics model 5900PR) produces a driving short-duration pulse of a width about 2.0 μs for the generating transducer. The generating transducer, placed far away from the sample to yield an input pulse approximating a plane wave, serves as the source of acoustic waves. A receiving transducer is placed on the opposite side of the sample and serves as the detector for the transmitted signal. Both the generating and receiving transducers have a diameter of 25 mm and a central frequency of 0.5 MHz. The assembly of the generating transducer, the sample, and the receiving transducer is immersed in a water tank. The corresponding correlation between the experimental mea-

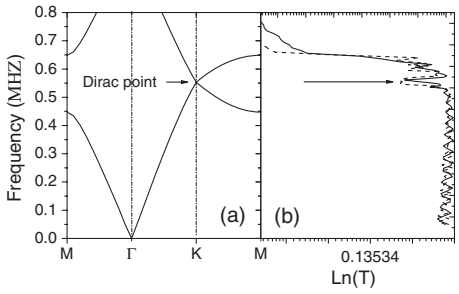

FIG. 1. (a) Calculated photonic band structure of acoustic wave for a triangular lattice of steel cylinder with $R/a = 1/3$ in a water background. (b) The measured transmission coefficient of acoustic wave along the ΓK direction for a 2D sonic crystal corresponding to (a). The solid line corresponds to the result with the sample thickness $L = 10a$ and the dashed line to that with $L = 20a$.

surements and the band structure can be observed. A dip region from 0.546 to 0.556 MHz [marked by an arrow in Fig. 1(b)] appears in the transmission spectrum, where the central frequency corresponds to the cross point of the band structure in Fig. 1(a).

The key feature of this band structure is that the band gap becomes vanishingly small at the corners of the Brillouin zone at $f = 0.55$ MHz, where two bands touch as a pair of cones in a linear fashion. This is similar to the case of the Dirac point of photons in the PCs although some asymmetric dispersion exists [1,2]. If we regard such a point as the Dirac point of an acoustic wave in the SC, the transport of the acoustic wave around it can be described by the following Dirac equation [1,2]:

$$\begin{pmatrix} 0 & -iv_D(\partial_x - i\partial_y) \\ -iv_D(\partial_x + i\partial_y) & 0 \end{pmatrix} \begin{pmatrix} \psi_1 \\ \psi_2 \end{pmatrix} = \delta\omega \begin{pmatrix} \psi_1 \\ \psi_2 \end{pmatrix}, \quad \delta\omega = \omega - \omega_D, \quad (1)$$

where $\psi = (\psi_1, \psi_2)$ represents the amplitudes of two degenerate Bloch states at one of the corners of the hexagonal first Brillouin zone. The frequency ω_D and velocity v_D in the Dirac point depend on the parameters of the SC. Thus, the flux of acoustic wave inside the SC can be written as $j_D = v_D(\psi_1^*\psi_2 + \psi_2^*\psi_1)$. In the free space outside of the SC, the transport of acoustic waves still follows the elastic wave equation. If the acoustic flux outside of the SC is defined as j_P, by applying the boundary condition of flux conservation ($j_P = j_D$) for the SC slabs with thickness L, we can obtain the transmission (T) of the acoustic wave around the Dirac point $T \propto 1/L$. This is further explained along with a detailed derivation in Ref. [2]. This means that the transmission of the acoustic wave near the Dirac point is inversely proportional to the thickness of the sample, which is similar to the diffusion behavior of waves through a disordered medium, even in the absence of any disorder in the SC.

In order to test such a phenomenon experimentally, we fabricated a series of SC slabs of different thicknesses and measured the transmission of acoustic waves through them. The widths of all samples are taken as 86 mm. The product of the transmission coefficient along the ΓK direction and L as a function of the sample thickness at $f = 0.55$ MHz is plotted in Fig. 2(b) as dark circle dots. The red solid line represents the numerical results obtained by a rigorous multiple-scattering method [6]. We find that the measured results from the experiment are generally in agreement with the calculated results. Both of them show that TL is an oscillating function of L. The axis of the oscillation is almost constant (green solid line) with the increase of L. Here the green solid line is drawn only for view, which can be regarded as corresponding to the above theoretical result ($T \propto 1/L$). The oscillating characteristics of TL depend on the interface and the thickness of the sample, which has been analyzed in Ref. [2]. That is to say, the transmission of the acoustic wave in such a case is actually inversely proportional to the thickness of the sample. Such an extremal transmission can appear only in small frequency intervals around the Dirac point (the dip region), which is similar to the case of electromagnetic waves in the PCs [2].

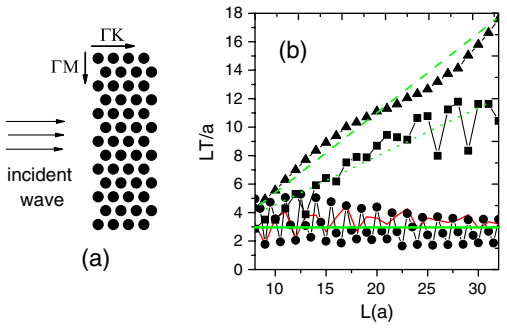

FIG. 2 (color online). (a) Schematic picture depicting measure processes. (b) The product of T and L as a function of sample thickness at different frequencies. Dark circle dots (experimental data) and the red line (numerical results) correspond to the case at $f = 0.55$ MHz. The dark square and triangular dots correspond to the experimental results at $f = 0.535$ and 0.45 MHz, respectively. The green lines (solid, dashed, and dotted) are drawn only for view. The green solid line can be regarded as corresponding to the theoretical result $T \propto 1/L$. The other parameters are identical to those in Fig. 1.

For comparison, at $f = 0.535$ MHz and $f = 0.45$ MHz we also give the experimental results away from the dip region as square and triangular dots in Fig. 2(b), respectively. It is seen clearly that they exhibit different features. At $f = 0.45$ MHz, the transmission coefficient is near constant where TL increases monotonously with L, which exhibits ballistic behavior. The feature of the transmission at $f = 0.535$ MHz is between the above two kinds of case, where it possesses both ballistic and diffusion behavior. At the same time, the transport behavior around the Dirac point is also different from the exponential decay with the increase of L, when the frequency lies in the gap regions. These can be seen more clearly in Fig. 3.

Figures 3(a) and 3(b) display the intensity distributions of the scattered fields at $f = 0.45$ and 0.55 MHz along the ΓK direction for the sample with $L = 20a$, respectively. The corresponding result at $f = 0.55$ MHz along the ΓM direction is shown in Fig. 3(c). The field intensities in the figures are over $20a \times 20a$ regions around the centers of the samples. X and Y present transverse and vertical directions of propagating waves, respectively. In the X direction, the field intensity in Fig. 3(a) does not decrease with the increase of L which corresponds to ballistic behavior, while it is suppressed exponentially in Fig. 3(c), because a gap exists. In contrast, the field intensity in Fig. 3(b) decreases linearly which is similar to the diffusion behavior of waves through a random medium. This means that the transport of acoustic waves near the Dirac point actually exhibits the phenomenon of extremal transmission.

After the phenomenon of extremal transmission was demonstrated, we investigated the dynamic behavior of

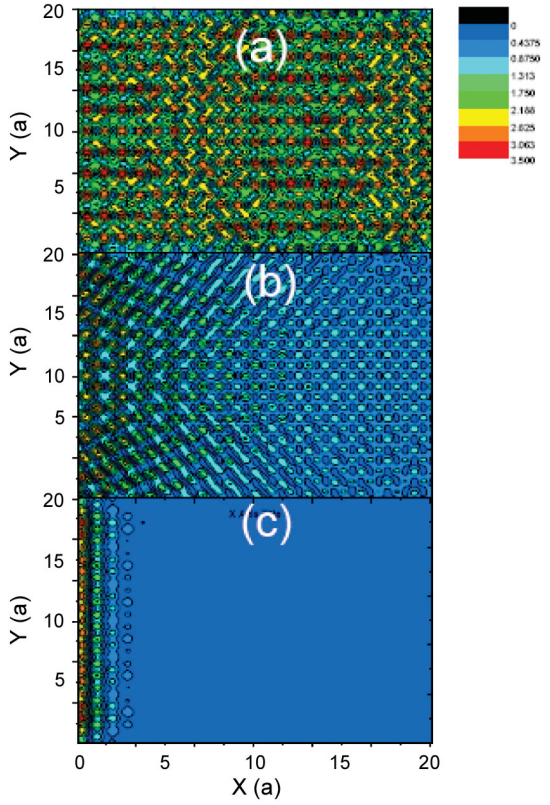

FIG. 3 (color). The field energy distribution at (a) $f = 0.45$ MHz and (b) $f = 0.55$ MHz along the ΓK direction and (c) at $f = 0.55$ MHz along the ΓM direction. The structure and parameter are the same as Fig. 2.

acoustic wave transport near the Dirac point in the above SC. Thus, we injected a Gaussian acoustic pulse into the samples and measured the time dependence of transmission through the sample. The measured results for filter frequency widths $\Delta f = 0.01$, 0.02, and 0.03 MHz are plotted in Figs. 4(a)–4(c). Dark, red, and green correspond

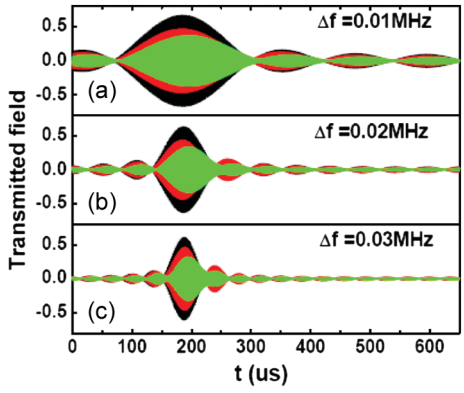

FIG. 4 (color). Experimental data of the transmission after the injection of a Gaussian pulse with center frequency $f = 0.55$ MHz into the samples. Dark, red, and green correspond to the cases with $L = 14a$, $19a$, and $24a$, respectively. (a), (b), and (c) correspond to the cases with the filter frequency widths $\Delta f = 0.01$, 0.02, and 0.03 MHz, respectively.

to the results with $L = 14a$, $19a$, and $24a$, respectively. It is clear that all of them are oscillations (beating effect). The oscillations have a transient character, as they are attenuated exponentially with the increase of time. They can be observed only when the thickness of the sample is bigger than several wavelengths. In addition, the period of oscillation depends weakly on the thickness of the sample, while it is linearly dependent on filter frequency widths. For example, the period for $\Delta f = 0.01$ MHz [in Fig. 4(a)] is nearly 3 times of that for $\Delta f = 0.03$ MHz [Fig. 4(c)].

Such a phenomenon is completely different from the oscillations of waves in a slab or cavity originating from the interface reflection or the Fabry-Perot effect [8,9]. It is caused by the interference between two linear modes around the Dirac point. In order to clarify the origin further, we studied the phase responses of the transmitted waves. The calculated and measured results for the sample with $L = 24a$ are plotted in Fig. 5(a) as a red solid line and a dark dot, respectively. The phase exhibits a linear relation for the frequencies away from the dip region such as $f = 0.45$ MHz (marked by a left arrow) very well. However, it twists around the Dirac point due to the interaction of waves between two modes (see the marked region by a right arrow), which leads to the oscillation of amplitude with time. In fact, such a phenomenon is also directly related to the ZB [10,11], which is similar to the case of electromagnetic waves [3].

According to the theory of ZB, the time-dependent displacement $[\bar{x}(t)]$ of the wave packet along the ΓK direction of the SC can be obtained analytically [see Eq. (7) in Ref. [3]]. After the average displacement is obtained, the velocity of the wave packet can be calculated by $\bar{v}(t) = \partial\bar{x}(t)/\partial t$. The calculated result for $\bar{v}(t)$ as a function of time is plotted in Fig. 5(b) as a solid line. Here $v_D = 0.6c$ is obtained experimentally, and the width of the wave packet is taken as corresponding to $\Delta f = 0.02$ MHz. It can be seen clearly that oscillation is a function of time, which is a direct manifestation of ZB. We can compare the oscillation for $\bar{v}(t)$ with the experimental results for the transmission coefficient, because the velocity of the wave packet is proportional to the rate of change of the energy flux $[j(t)]$ of the acoustic pulse $[j(t) \propto \bar{v}(t)]$. At the same time, $j(t)$ is a time-derivative of the pulse intensity $[I(t)]$ $[j(t) = dI(t)/dt]$. The intensity $[I(t)]$ or transmission coefficient can be obtained from experimental measurements (see Fig. 4). Thus, we can obtain $j(t)$ from the experimental data and quantitatively compare it with the theoretical result for $\bar{v}(t)$.

Dark circle dots and triangular dots in Fig. 5(b) represent the experimental results of $j(t)$ for $\Delta f = 0.02$ MHz at $L = 14a$ and $24a$, respectively. Here the data are taken only for one period [between the second peak and the third peak in Fig. 4(b)]. The dashed line and the dotted line are the corresponding numerical results based on the multiple-scattering method [6]. The agreements between them are observed again. Comparing them with a solid line [theoretical result for $\bar{v}(t)$], we find that the oscillating periods

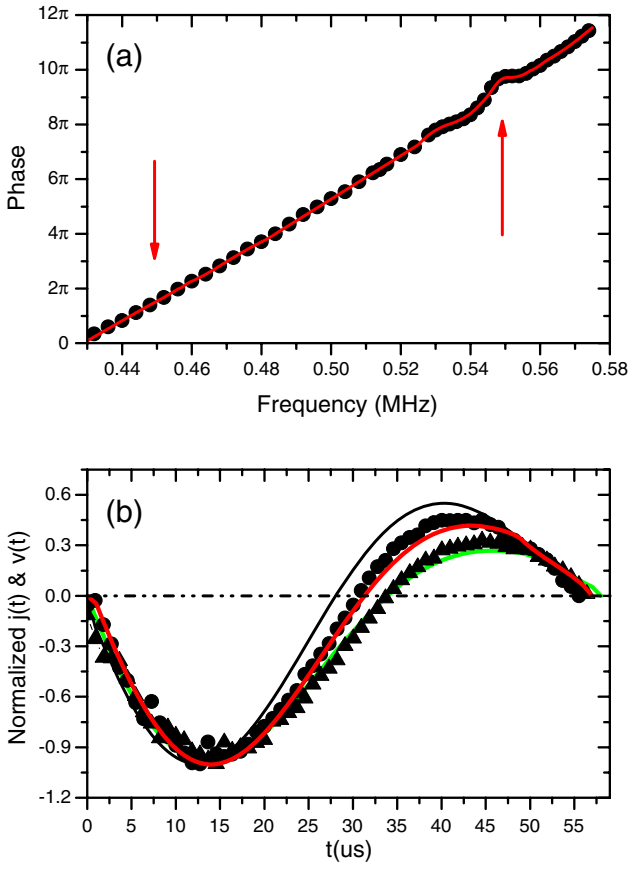

FIG. 5 (color online). (a) The phase of transmission wave as a function of frequency for the sample with $L = 24a$. The solid line and dark circle dots correspond to the numerical results and experimental data, respectively. (b) Comparison between the theoretical result (solid line) for velocity $[\bar{v}(t)]$ of pulse evolution and experimental measurements (circle, triangular dots) for the rate of change of the energy flux $j(t)$. Triangular and circle dots correspond to the cases with $L = 14a$ and $24a$ for the filter frequency widths $\Delta f = 0.02$ MHz, respectively. Here the dashed line (red) and the dotted line (green) are the corresponding numerical results for two kinds of cases, respectively.

are basically in agreement. Some differences between the theoretical results and experimental measurements originate from the effect of finite size and interface as has been analyzed above. In addition, the deficiency of the oscillation for the thin samples can also be explained by the theory of ZB. When the thickness of the sample is very small, the transport of waves exhibits ballistic behavior. In this case, it cannot be described by Eq. (1). Therefore, the oscillation disappears. Essentially, all phenomena observed in the experiments can be explained by the theory of ZB. This means that the beating effect observed from the experimental measurements is an acoustic analogue effect to the ZB of relativistic electrons, which is similar to the case of electromagnetic waves in the PCs [3] or electrons in the monolayer graphene [12–14]. The above experiments and calculations focus on only one kind of structure parameters of the SC. In fact, we have also considered other cases with different structure parameters, for example, the radius of steel cylinder change from $0.3a$ to $0.4a$. Similar phenomena have been obtained.

In summary, we have demonstrated experimentally the existence of a new transport regime of acoustic waves in the SC near the Dirac point. In this regime, the transmission of acoustic waves is inversely proportional to the thickness of the sample, which can be described by the Dirac equation adequately. Based on these, we have directly observed an acoustic analogue effect to the ZB of relativistic electrons from experimental measurements for the time dependence of transmission coefficients of acoustic pulses. We anticipate our work to be a starting point for more experimental investigations on the phenomena of relativistic quantum mechanics, by using classical waves and extensive application of the phenomena to acoustic devices.

This work was supported by the National Natural Science Foundation of China (Grants No. 10825416 and No. 50425206) and the National Key Basic Research Special Foundation of China (Grant No. 2007CB613205).

[1] F. D. M. Haldane and S. Raghu, Phys. Rev. Lett. **100**, 013904 (2008); S. Raghu and F. D. M. Haldane, Phys. Rev. A **78**, 033834 (2008).
[2] R. A. Sepkhanov, Ya. B. Bazaliy, and C. W. J. Beenakker, Phys. Rev. A **75**, 063813 (2007); X. D. Zhang, Phys. Lett. A **372**, 3512 (2008).
[3] X. D. Zhang, Phys. Rev. Lett. **100**, 113903 (2008).
[4] K. S. Novoselov, A. K. Geim, S. V. Morozov, D. Jiang, Y. Zhang, S. V. Dubonos, I. V. Grigorieva, and A. A. Firsov, Science **306**, 666 (2004).
[5] T. Ando, J. Phys. Soc. Jpn. **74**, 777 (2005).
[6] J. Mei, Z. Liu, J. Shi, and D. Tian, Phys. Rev. B **67**, 245107 (2003); Y. Lai, X. Zhang, and Z. Q. Zhang, Appl. Phys. Lett. **79**, 3224 (2001).
[7] M. Ke, Z. He, S. Peng, Z. Liu, J. Shi, W. Wen, and P. Sheng, Phys. Rev. Lett. **99**, 044301 (2007).
[8] H. Sanchis-Alepuz, Y. A. Kosevich, and J. Sanchez-Dehesa, Phys. Rev. Lett. **98**, 134301 (2007).
[9] Z. He, S. Peng, F. Cai, M. Ke, and Z. Liu, Phys. Rev. E **76**, 056605 (2007).
[10] E. Schrödinger, Sitzungsber. Preuss. Akad. Wiss. Phys. Math. Kl. **24**, 418 (1930).
[11] W. Zawadzki, Phys. Rev. B **72**, 085217 (2005); T. M. Rusin and W. Zawadzki, J. Phys. Condens. Matter **19**, 136219 (2007).
[12] M. I. Katsnelson, Eur. Phys. J. B **51**, 157 (2006).
[13] J. Cserti and G. David, Phys. Rev. B **74**, 172305 (2006).
[14] T. M. Rusin and W. Zawadzki, Phys. Rev. B **76**, 195439 (2007).